Lower critical fields of superconducting $PrFeAsO_{1-y}$ single crystals

R. Okazaki,[1] M. Konczykowski,[2] C. J. van der Beek,[2] T. Kato,[1] K. Hashimoto,[1] M. Shimozawa,[1] H. Shishido,[1] M. Yamashita,[1] M. Ishikado,[3] H. Kito,[4,5] A. Iyo,[4,5] H. Eisaki,[4,5] S. Shamoto,[3,5] T. Shibauchi,[1] and Y. Matsuda[1,2]
[1]*Department of Physics, Kyoto University, Kyoto 606-8502, Japan*
[2]*Laboratorie des Solides Irradiés, CNRS-UMR 7642 & CEA/DSM/IRAMIS, Ecole Polytechnique, 91128 Palaiseau, France*
[3]*Quantum Beam Science Directorate, Japan Atomic Energy Agency, Tokai, Naka, Ibaraki 319-1195, Japan*
[4]*Nanoelectronics Research Institute (NeRI), National Institute of Advanced Industrial Science and Technology (AIST), 1-1-1 Central 2, Umezono, Tsukuba, Ibaraki 305-8568, Japan*
[5]*JST, TRIP, Chiyoda, Tokyo 102-0075, Japan*
(Received 22 November 2008; published 19 February 2009)

We have studied the lower critical fields H_{c1} of superconducting iron oxipnictide $PrFeAsO_{1-y}$ single crystals for $\boldsymbol{H}$ parallel and perpendicular to the ab planes. Measurements of the local magnetic induction at positions straddling the sample edge by using a miniature Hall-sensor array clearly resolve the first flux penetration from the Meissner state. The temperature dependence of H_{c1} for $\boldsymbol{H} \parallel c$ is well scaled by the in-plane penetration depth without showing any unusual behavior, in contrast to previous reports. The anisotropy of penetration lengths at low temperatures is estimated to be $\simeq 2.5$, which is considerably smaller than the anisotropy of the coherence lengths. This is indicative of multiband superconductivity in this system in which the active band for superconductivity is more anisotropic. We also point out that the local induction measured at a position near the center of the crystal, which has been used in a number of reports for the determination of H_{c1}, might seriously overestimate the obtained H_{c1} value.

DOI: 10.1103/PhysRevB.79.064520 PACS number(s): 74.25.Bt, 74.25.Dw, 74.25.Op, 74.70.−b

I. INTRODUCTION

The recent discovery of high-temperature superconductivity in Fe-based compounds has attracted considerable interest.[1] In this new class of compounds with a very low carrier density,[2–9] superconductivity occurs in proximity to a magnetic instability, and unconventional pairing mechanisms mediated by magnetic fluctuations have been proposed by several groups.[10–12] One of the remarkable features, which is in sharp contrast to the high-T_c cuprates, appears to be the multiband nature of superconductivity, in electron and hole pockets.[13] Recently, a multiband effect on superconductivity has been reported in several compounds.[14–16] In particular, the two-gap superconductivity in MgB_2 manifests itself in the unusual temperature and magnetic field dependence of the anisotropy parameters in the superconducting state.[17–19] However, the crucial difference is that the interband coupling is very weak in MgB_2, while in Fe-based compounds nesting between the hole and electron bands was suggested to be important for the occurrence of high-temperature superconductivity.[10–12,20–23] In this context, a detailed clarification of the multiband nature of superconductivity in the Fe-based oxypnictides is indispensable for the elucidation of the superconducting properties, and especially for the pairing mechanism.

An accurate determination of the lower critical field H_{c1} is an important means to clarify not only the superconducting gap symmetry but also the multiband nature of superconductivity. However, the reliable measurement of the lower critical field is a difficult task, in particular when strong vortex pinning is present. We also point out that to date the reported values of anisotropy parameter strongly vary,[24–27] spanning from 1.2 (Ref. 27) up to ~20 (Ref. 24), which may be partly due to the effects of strong pinning. In this study, we use an unambiguous method to avoid this difficulty associated with pinning by determining H_{c1} as the field H_p at which first flux penetration occurs from the edge of the crystal. This allows us to extract the temperature-dependent values of the lower critical fields parallel to the c axis (H_{c1}^{c}) and the ab plane (H_{c1}^{ab}), respectively, as well as the anisotropy parameter H_{c1}^{c}/H_{c1}^{ab} in single crystals of Fe-based superconductors.

We directly determine H_p by measuring the magnetic induction just inside and outside the edge of the single crystals, by using a miniature Hall-sensor array. First, we show that local magnetization measurements at a position near the center of the crystal, which have been used by several groups for the determination of H_{c1}, seriously overestimate H_{c1} in systems with strong pinning. Second, we find that the temperature dependence of H_{c1} determined at the edge does not show any unusual behavior[28] and is well scaled by the penetration depth results measured on the crystal in the same batch.[29] Finally, we find that the anisotropy of the penetration depths $\gamma_\lambda \equiv \lambda_c/\lambda_{ab} \simeq H_{c1}^{c}/H_{c1}^{ab}$, where λ_c and λ_{ab} are out-of-plane and in-plane penetration depths, respectively, is much smaller than the anisotropy of the coherence lengths $\gamma_\xi \equiv \xi_{ab}/\xi_c = H_{c2}^{ab}/H_{c2}^{c}$, where ξ_{ab} and ξ_c are in- and out-of-plane coherence lengths, respectively, and H_{c2}^{ab} and H_{c2}^{c} are the upper critical fields parallel and perpendicular to the ab plane, respectively. This result provides strong evidence for the multiband nature of the superconductivity.

II. EXPERIMENTAL

Experiments have been performed on high-quality $PrFeAsO_{1-y}$ single crystals, grown by a high-pressure synthesis method using a belt-type anvil apparatus (Riken CAP-07). Powders of PrAs, Fe, and Fe_2O_3 were used as the starting materials. PrAs was obtained by reacting Pr chips and As

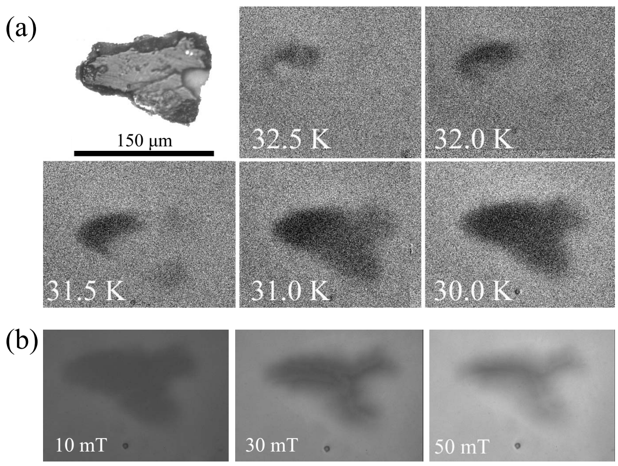

FIG. 1. (a) Differential magneto-optics images of $PrFeAsO_{1-y}$ 1 with field modulation $\delta B = 0.2$ mT in zero field. The Meissner screening occurs completely within narrow temperature range. (b) MO images at $T = 7.1$ K. Magnetic flux penetrates from the edge of the crystal, and the field distribution shows the Bean critical state.

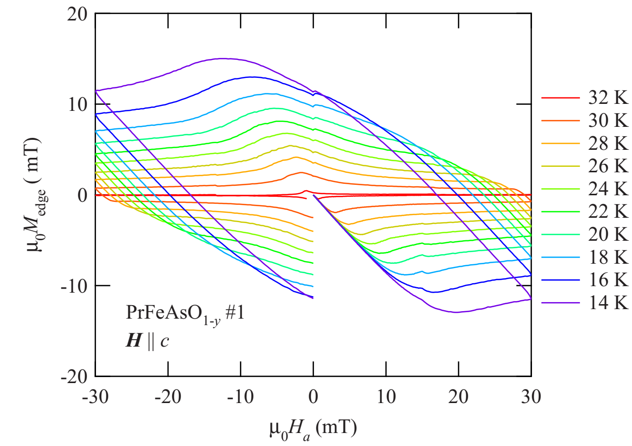

FIG. 2. (Color online) Local magnetization loops for $\boldsymbol{H} \| c$, measured by the miniature Hall sensor located at ≤ 10 μm from the edge of the crystal.

pieces at 500 °C for 10 h, followed by a treatment at 850 °C for 5 h in an evacuated quartz tube. The starting materials were mixed at nominal compositions of $PrFeAsO_{0.6}$ and ground in an agate mortar in a glove box filled with dry nitrogen gas. The mixed powders were pressed into pellets. The samples were then grown by heating the pellets in BN crucibles under a pressure of about 2 GPa at 1300 °C for 2 h. Plateletlike single crystals of dimensions up to $150 \times 150 \times 30$ μm^3 were mechanically selected from the polycrystalline pellets. The single crystalline nature of the samples was checked by Laue x-ray diffraction.[30] Our crystals, whose T_c (≈ 34 K) is lower than the optimum $T_c \approx 51$ K of $PrFeAsO_{1-y}$,[31] are in the underdoped regime ($y \sim 0.1$),[32] which is close to the spin-density-wave order.[33] The sample homogeneity was checked by magneto-optical (MO) imaging. MO images of $PrFeAsO_{1-y}$ sample 1 ($\sim 135 \times 63 \times 18$ μm^3) are shown in Fig. 1(a). The crystal exhibits a nearly perfect Meissner state ~ 2 K below T_c; no weak links are observed, indicating a good homogeneity. At low temperatures, the magnetic field distribution is well described by the Bean critical state model as shown in Fig. 1(b).[34]

The local induction near the surface of the platelet crystal has been measured by placing the sample on top of a miniature Hall-sensor array tailored in a GaAs/AlGaAs heterostructure.[35] Each Hall sensor has an active area of 3×3 μm^2; the center-to-center distance of neighboring sensors is 20 μm. The local induction at the edge of the crystal was detected by the miniature Hall sensor located at ≤ 10 μm from the edge. The magnetic field H_a is applied for $\boldsymbol{H} \| c$ and $\boldsymbol{H} \| ab$ planes by using a low-inductance 2.4 T superconducting magnet with a negligibly small remanent field.

The in-plane resistivity is measured by the standard four-probe method under magnetic fields up to 10 T. The electrical contacts were attached by using the W deposition technique in a focused-ion-beam system.

III. RESULTS AND DISCUSSION

In Fig. 2 we show the field dependence of the "local magnetization," $M_{edge} \equiv \mu_0^{-1} B_{edge} - H_a$, at the edge of the crystal, for $\boldsymbol{H} \| c$, measured after zero-field cooling (ZFC). After the initial negative slope corresponding to the Meissner state, vortices enter the sample and $M_{edge}(H_a)$ shows a large hysteresis. The shape of the magnetization loops (almost symmetric about the horizontal axis) indicates that the hysteresis mainly arises from bulk flux pinning rather than from the (Bean-Livingston) surface barrier.[36]

As shown in Fig. 2, the initial slope of the magnetization exhibits a nearly perfect linear dependence, $M_{edge} = -\alpha H_a$. Since the Hall sensor is placed on the top surface, with a small but nonvanishing distance between the sensor and the crystal, the magnetic field leaks around the sample edge with the result that the slope α is slightly smaller than unity. Figure 3 shows typical curves of $B^{1/2} \equiv \mu_0^{1/2}(M + \alpha H_a)^{1/2}$ at the

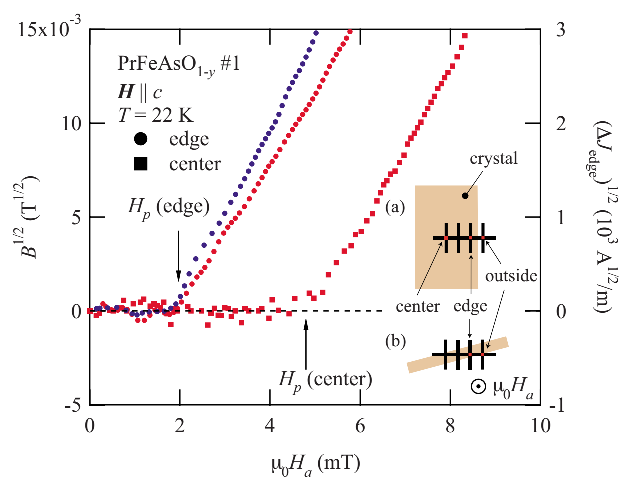

FIG. 3. (Color online) Typical curves of $\sqrt{B}$ (left axis) at the edge (circles) and at the center (squares) of the crystal and $\sqrt{\Delta j_{edge}}$ (right axis) plotted as a function of H_a for $\boldsymbol{H} \| c$ at $T = 22$ K in which H_a is increased after ZFC. The insets are schematic illustrations of the experimental setup for (a) $\boldsymbol{H} \| c$ and (b) $\boldsymbol{H} \| ab$ planes.

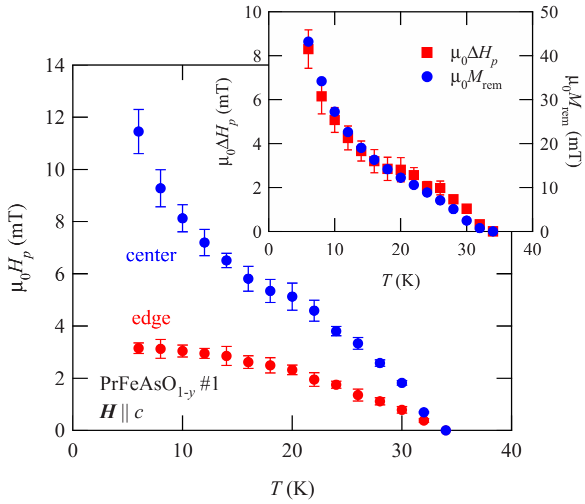

FIG. 4. (Color online) The temperature dependence of the flux penetration fields H_p at the edge and the center of the crystal. The inset shows the temperature dependence of the difference between H_p in the center and at the edge (left axis), as well as the remanent magnetization M_{rem} (right axis).

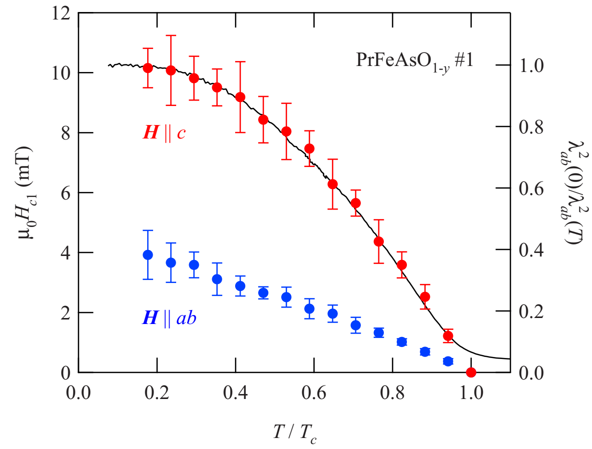

FIG. 5. (Color online) Lower critical fields as a function of temperature in PrFeAsO$_{1-y}$ single crystals (left axis). The solid line (right axis) presents the superfluid density $\lambda_{ab}^2(0)/\lambda_{ab}^2(T)$ determined by surface impedance measurements on crystals from the same batch (Ref. 29).

edge (circles) and at the center (squares) of the crystal, plotted as a function of H_a; the external field orientation $\boldsymbol{H}\parallel c$ and $T=22$ K. The αH_a term is obtained by a least-squares fit of the low-field magnetization. The first penetration field H_p corresponding to the field H_p (edge), above which $B^{1/2}$ increases almost linearly, is clearly resolved. In Fig. 3, we show the equivalent curve, measured at the center of the crystal. At the center, $B^{1/2}$ also increases linearly, starting from a larger field, H_p (center).

We have measured the positional dependence of H_p and observed that it increases with increasing distance from the edge. To examine whether H_p (edge), i.e., H_p measured at ≤ 10 μm from the edge, truly corresponds to the field of first flux penetration at the boundary of the crystal, we have determined the local screening current density $j_{\text{edge}}=\mu_0^{-1}(B_{\text{edge}}-B_{\text{outside}})/\Delta x$ at the crystal boundary. Here B_{edge} is the local magnetic induction measured by the sensor just inside the edge, and B_{outside} is the induction measured by the neighboring sensor just outside the edge. For fields less than the first penetration field, $j_{\text{edge}}\simeq\beta H_a$ is the Meissner current, which is simply proportional to the applied field (β is a constant determined by geometry). At H_p, the screening current starts to deviate from linearity. Figure 3 shows the deviation $\Delta j_{\text{edge}}\equiv j_{\text{edge}}-\beta H_a$ as a function of H_a. As depicted in Fig. 3, $\sqrt{\Delta j_{\text{edge}}}$ again increases linearly with H_a above H_p (edge). This indicates that the H_p (edge) is very close to the true field of first flux penetration.

In Fig. 4, we compare the temperature dependence of H_p (edge) and H_p (center). In the whole temperature range, H_p (center) well exceeds H_p (edge). Moreover, H_p (center) increases with decreasing T without any tendency toward saturation. In sharp contrast, H_p (edge) saturates at low temperatures. The inset of Fig. 4 shows the difference between H_p measured in the center and at the edge: $\Delta H_p=H_p$ (center); $-H_p$ (edge). ΔH_p increases steeply with decreasing temperature. Also plotted in the inset of Fig. 4 is the remanent magnetization M_{rem} (i.e., the $H_a=0$ value of M_{edge} on the decreasing field branch) measured at near the crystal center. This is proportional to the critical current density j_c arising from flux pinning. The temperature dependence of ΔH_p is very similar to that of j_c, which indicates that H_p (center) is strongly influenced by pinning. Hence, the present results demonstrate that the lower critical field value determined by local magnetization measurements carried out at positions close to the crystal center, such as reported by several groups, is affected by vortex pinning effects and might be seriously overestimated.[28,37]

The absolute value of H_{c1} is evaluated by taking into account the demagnetizing effect. For a platelet sample, H_{c1} is given by

$$H_{c1} = H_p/\tanh\sqrt{0.36b/a}, \tag{1}$$

where a and b are the width and the thickness of the crystal, respectively.[38] In the situation where $\boldsymbol{H}\parallel c$, $a=63$ μm and $b=18$ μm, while $a=18$ μm and $b=63$ μm for $\boldsymbol{H}\parallel ab$ plane. These values yield $H_{c1}^c=3.22H_p$ and $H_{c1}^{ab}=1.24H_p$, respectively. In Fig. 5, we plot H_{c1} as a function of temperature both for $\boldsymbol{H}\parallel c$ and $\boldsymbol{H}\parallel ab$ planes. The solid line in Fig. 5 indicates the temperature dependence of the superfluid density normalized by the value at $T=0$ K, which is obtained from ab-plane penetration depth measurements of a sample from the same batch.[29] $H_{c1}^c(T)$ is well scaled by the superfluid density, which is consistent with fully gapped superconductivity; it does not show the unusual behavior reported in Ref. 28. To roughly estimate the in-plane penetration depth at low temperatures, we use the approximate single-band London formula

$$\mu_0 H_{c1}^c = \frac{\Phi_0}{4\pi\lambda_{ab}^2}\left[\ln\frac{\lambda_{ab}}{\xi_{ab}} + 0.5\right], \tag{2}$$

where Φ_0 is the flux quantum. Using $\ln \lambda_{ab}/\xi_{ab}+0.5\sim 5$, we obtain $\lambda_{ab}\sim 280$ nm. This value is in close correspondence

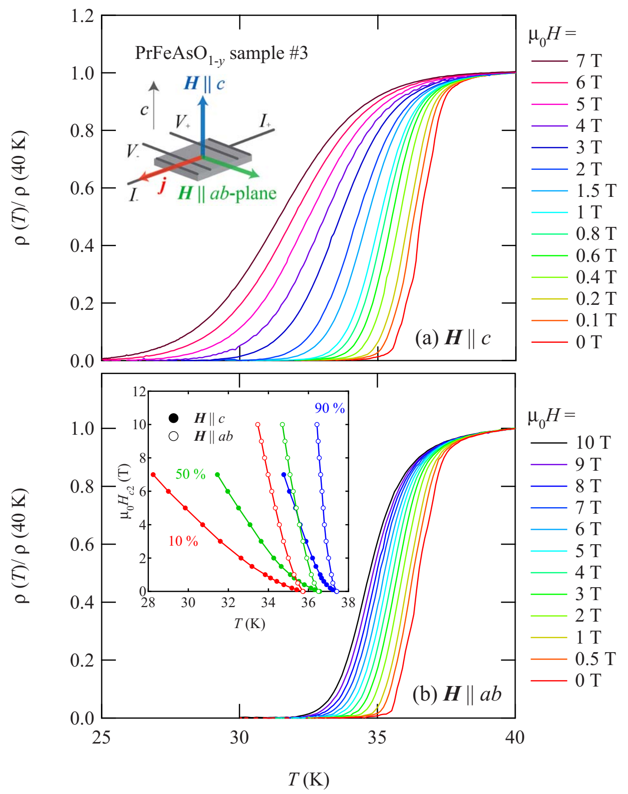

FIG. 6. (Color online) Temperature dependence of the in-plane resistivity in $PrFeAsO_{1-y}$ single crystals for (a) $\boldsymbol{H}\|c$ and (b) $\boldsymbol{H}\|ab$ planes. Inset shows the temperature dependence of the upper critical fields H_{c2} determined by several criteria that the resistivity reaches 10%, 50%, and 90% of the normal-state resistivity. The experimental configuration is also sketched.

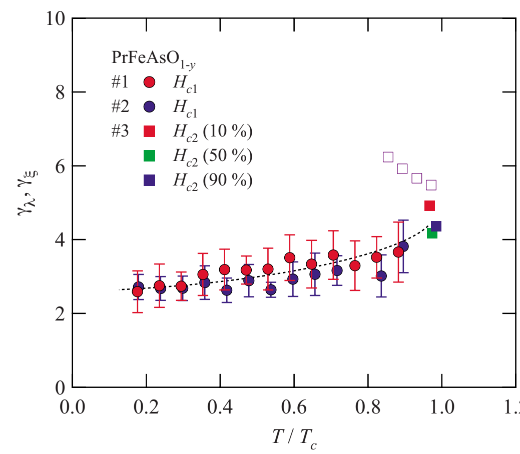

FIG. 7. (Color online) Normalized temperature dependence of the anisotropies of H_{c1} (γ_λ, closed circles) and H_{c2} (γ_ξ, closed squares) in $PrFeAsO_{1-y}$ single crystals. The anisotropy of H_{c2} in $NdFeAsO_{0.82}F_{0.18}$ (γ_ξ, open squares) measured by Y. Jia *et al.* (Ref. 42) is also plotted. The dashed line is a guide to the eyes.

with the muon-spin-relaxation (μSR) results in slightly underdoped LaFeAs(O,F).[39]

Figures 6(a) and 6(b) depict the temperature dependence of the in-plane resistivity for $\boldsymbol{H}\|c$ and $\boldsymbol{H}\|ab$ planes, respectively. In the inset of Fig. 6(b), we display the fields at which the resistivity is equal to 10%, 50%, and 90% of the normal-state resistivity. For sufficiently high magnetic field, these resistance loci are roughly proportional to the upper critical field. In zero field, the resistive transition exhibits a rather sharp transition with the transition width $\Delta T_c \approx 2$ K. By applying a magnetic field along the c axis, the transition shifts to slightly lower temperatures and becomes broadened. The resistive transition curves broaden less for $\boldsymbol{H}\|ab$ plane. These results indicate that the anisotropy of the upper critical fields in the present system is rather large and that fluctuation effects play an important role for the transition in magnetic fields,[40] similar to high-T_c cuprates.[41]

Finally, Fig. 7 shows the anisotropy of the lower critical fields, γ_λ obtained from the results in Fig. 5. Here, since the penetration lengths are much larger than the coherence lengths for both $\boldsymbol{H}\|ab$ and $\boldsymbol{H}\|c$, the logarithmic term in Eq. (2) does not strongly depend on the direction of magnetic field. We thus assumed $H_{c1}^{c}/H_{c1}^{ab} \simeq \lambda_c/\lambda_{ab}$. The anisotropy $\gamma_\lambda \approx 2.5$ at very low temperature and increases gradually with temperature. In Fig. 7, the anisotropy of the upper critical fields γ_ξ is also plotted, where γ_ξ is determined by the loci of 10%, 50%, and 90% of the normal-state resistivity [see the inset of Fig. 6(b)]. Since H_{c2} increases rapidly and well exceeds 10 T just below T_c for $\boldsymbol{H}\|ab$, plotting γ_ξ is restricted to a narrow temperature interval. In Fig. 7, we also plot the H_{c2}-anisotropy data measured on $NdFeAsO_{0.82}F_{0.18}$ by Jia *et al.*[42] These indicate that the temperature dependence of γ_λ is markedly different from that of γ_ξ.

According to the anisotropic Ginzburg-Landau (GL) equation in single-band superconductors, γ_λ should coincide with γ_ξ over the whole temperature range. Therefore, the large difference between these anisotropies provides strong evidence for multiband superconductivity in the present system. We discuss the anisotropy parameters for the multiband superconductivity below. According to GL theory, γ_λ and γ_ξ at T_c are given as

$$\gamma_\xi^2(T_c) = \gamma_\lambda^2(T_c) = \frac{\langle \Omega^2 v_a^2 \rangle}{\langle \Omega^2 v_c^2 \rangle}, \tag{3}$$

where $\langle \cdots \rangle$ denotes the average over the Fermi surface v_a and v_c are the Fermi velocities parallel and perpendicular to the ab plane, respectively.[43,44] Ω represents the gap anisotropy ($\langle \Omega^2 \rangle = 1$), which is related to the pair potential $V(\boldsymbol{v},\boldsymbol{v}') = V_0 \Omega(\boldsymbol{v}) \Omega(\boldsymbol{v}')$. At $T=0$ K, the anisotropy of the penetration depths is

$$\gamma_\lambda^2(0) = \frac{\langle v_a^2 \rangle}{\langle v_c^2 \rangle}. \tag{4}$$

The gap anisotropy does not enter $\gamma_\lambda(0)$, while γ_ξ at $T=0$ K is mainly determined by the gap anisotropy of the active band responsible for superconductivity. Thus the gradual reduction in γ_λ with decreasing temperature can be accounted for by considering that the contribution of the gap anisotropy diminished at low temperatures. This also implies that the superfluid density along the c axis $\lambda_c^2(0)/\lambda_c^2(T)$ has steeper temperature dependence than that in the plane $\lambda_{ab}^2(0)/\lambda_{ab}^2(T)$. A pronounced discrepancy between γ_ξ and γ_λ provides strong evidence for the multiband nature of superconductivity in $PrFeAsO_{1-y}$, with different gap values in different bands. We note that similar differences between $\gamma_\xi(T)$ and $\gamma_\lambda(T)$, as well as $\lambda_c^2(0)/\lambda_c^2(T)$ and $\lambda_{ab}^2(0)/\lambda_{ab}^2(T)$, have been reported in the two-gap superconductor MgB_2.[18,19] We also note that angle-resolved photoemission spectroscopy (ARPES),[45] Andreev reflection,[46] and penetration depth[47] measurements on $(K_{1-x}Ba_x)Fe_2As_2$ and NMR (Ref. 48) and penetration depth[49] studies of LnFeAs(O,F) (Ln=Pr,Sm) have suggested multiband superconductivity with two gap values in Fe-based oxypnictides.

Band-structure calculations for $LaFeAsO_{1-x}F_x$ yield an anisotropy of the resistivity of approximately 15 for isotropic scattering,[13] which corresponds to $\gamma_\lambda \sim 4$. This value is close to the observed value. The fact that γ_ξ well exceeds γ_λ indicates that the active band for superconductivity is more anisotropic than the passive band. According to band-structure calculations, there are five relevant bands in $LaFeAsO_{1-x}F_x$. Among them, one of the three hole bands near the Γ point and the two electron bands near the M point are two dimensional and cylindrical. The other two hole bands near the Γ point have more dispersion along the c axis,[13] although the shape of these Fermi surfaces is sensitive to the position of the As atom with respect to the Fe plane, which in turn depends on the rare earth.[50] Our results implying that the active band is more anisotropic are in good correspondence with the view that the nesting between the cylindrical hole and electron Fermi surfaces is essential for superconductivity. This is expected to make these two-dimensional bands the active ones, with a large gap, and the other more three-dimensional bands passive ones with smaller gaps.

IV. SUMMARY

In summary, we have measured the lower critical field H_{c1} in $PrFeAsO_{1-y}$ single crystals for $\boldsymbol{H}\parallel c$ and $\boldsymbol{H}\parallel ab$ planes by utilizing an array of miniature Hall sensor. Conventional methods using a single micro-Hall probe placed on the center of the crystal might overestimate H_{c1} due to strong flux pinning. H_{c1} measured by the sensor located very near to the edge of the crystal shows saturating behavior at low temperatures, which is consistent with the previous reports on the penetration depth measurements. The anisotropy of H_{c1} slightly decreases with decreasing temperature and is indicative of multiband superconductivity in $PrFeAsO_{1-y}$ in which the active band for superconductivity is more anisotropic.

Note added. Recently, H_{c1} measurements on NdFeAs(O,F) by using Hall probes are reported,[51] which show similar temperature dependence of H_{c1}.

ACKNOWLEDGMENTS

We thank A. E. Koshelev for useful discussion and T. Terashima for technical assistance. This work was supported through Contract No. KAKENHI 20224008 from JSPS by Grant-in-Aid for the Global COE program "The Next Generation of Physics, Spun from Universality and Emergence" and by Grant-in-Aid for Specially Promoted Research No. 17001001 from MEXT, Japan. R.O. and H.S. were supported by the JSPS Research Foundation for Young Scientists.

[1] Y. Kamihara, T. Watanabe, M. Hirano, and H. Hosono, J. Am. Chem. Soc. **130**, 3296 (2008).
[2] H. Takahashi, K. Igawa, K. Arii, Y. Kamihara, M. Hirano, and H. Hosono, Nature (London) **453**, 376 (2008).
[3] G. F. Chen, Z. Li, D. Wu, G. Li, W. Z. Hu, J. Dong, P. Zheng, J. L. Luo, and N. L. Wang, Phys. Rev. Lett. **100**, 247002 (2008).
[4] Z.-A. Ren, J. Yang, W. Lu, W. Yi, G.-C. Che, X.-L. Dong, L.-L. Sung, and Z.-X. Zhao, Mater. Res. Innovations **12**, 105 (2008).
[5] H. Kito, H. Eisaki, and A. Iyo, J. Phys. Soc. Jpn. **77**, 063707 (2008).
[6] Z.-A. Ren, J. Yang, W. Lu, W. Yi, X.-L. Shen, Z.-C. Li, G.-C. Che, X.-L. Dong, L.-L. Sung, F. Zhou, and Z.-X. Zhao, Europhys. Lett. **82**, 57002 (2008).
[7] X. H. Chen, T. Wu, G. Wu, R. H. Liu, H. Chen, and D. F. Fang, Nature (London) **453**, 761 (2008).
[8] J. Yang, Z.-C. Li, W. Lu, W. Yi, X.-L. Shen, Z.-A. Ren, G.-C. Che, X.-L. Dong, L.-L. Sun, F. Zhou, and Z.-X. Zhao, Supercond. Sci. Technol. **21**, 082001 (2008).
[9] C. Wang, L. Li, S. Chi, Z. Zhu, Z. Ren, Y. Li, Y. Wang, X. Lin, Y. Luo, S. Jiang, X. Xu, G. Cao, and Z. Xu, Europhys. Lett. **83**, 67006 (2008).
[10] I. I. Mazin, D. J. Singh, M. D. Johannes, and M. H. Du, Phys. Rev. Lett. **101**, 057003 (2008).
[11] K. Kuroki, S. Onari, R. Arita, H. Usui, Y. Tanaka, H. Kontani, and H. Aoki, Phys. Rev. Lett. **101**, 087004 (2008).
[12] H. Aoki, arXiv:0811.1656 (unpublished).
[13] D. J. Singh and M.-H. Du, Phys. Rev. Lett. **100**, 237003 (2008).
[14] G. Seyfarth, J. P. Brison, M.-A. Méasson, J. Flouquet, K. Izawa, Y. Matsuda, H. Sugawara, and H. Sato, Phys. Rev. Lett. **95**, 107004 (2005).
[15] Y. Kasahara, T. Iwasawa, H. Shishido, T. Shibauchi, K. Behnia, Y. Haga, T. D. Matsuda, Y. Onuki, M. Sigrist, and Y. Matsuda, Phys. Rev. Lett. **99**, 116402 (2007).
[16] Y. Nakajima, T. Nakagawa, T. Tamegai, and H. Harima, Phys. Rev. Lett. **100**, 157001 (2008).
[17] F. Bouquet, Y. Wang, I. Sheikin, T. Plackowski, A. Junod, S. Lee, and S. Tajima, Phys. Rev. Lett. **89**, 257001 (2002).
[18] L. Lyard, P. Szabo, T. Klein, J. Marcus, C. Marcenat, K. H. Kim, B. W. Kang, H. S. Lee, and S. I. Lee, Phys. Rev. Lett. **92**, 057001 (2004).
[19] J. D. Fletcher, A. Carrington, O. J. Taylor, S. M. Kazakov, and J. Karpinski, Phys. Rev. Lett. **95**, 097005 (2005).
[20] V. Cvetkovic and Z. Tesanovic, Europhys. Lett. **85**, 37002 (2009).
[21] K. Seo, B. A. Bernevig, and J. Hu, Phys. Rev. Lett. **101**, 206404 (2008).
[22] H. Ikeda, J. Phys. Soc. Jpn. **77**, 123707 (2008).
[23] T. Nomura, arXiv:0811.2462 (unpublished).
[24] S. Weyeneth, R. Puzniak, U. Mosele, N. D. Zhigadlo, S. Katrych, Z. Bukowski, J. Karpinski, S. Kohout, J. Roos, and H. Keller, arXiv:0806.1024, J. Supercond. Novel Magn. (to be published).

[25] C. Martin, R. T. Gordon, M. A. Tanatar, M. D. Vannette, M. E. Tillman, E. D. Mun, P. C. Canfield, V. G. Kogan, G. D. Samolyuk, J. Schmalian, and R. Prozorov, arXiv:0807.0876 (unpublished).
[26] L. Balicas, A. Gurevich, Y. J. Jo, J. Jaroszynski, D. C. Larbalestier, R. H. Liu, H. Chen, X. H. Chen, N. D. Zhigadlo, S. Katrych, Z. Bukowski, and J. Karpinski, arXiv:0809.4223 (unpublished).
[27] D. Kubota, T. Ishida, M. Ishikado, S. Shamoto, H. Kito, A. Iyo, and H. Eisaki, arXiv:0810.5623 (unpublished).
[28] C. Ren, Z.-S. Wang, H. Yang, X. Zhu, L. Fang, G. Mu, L. Shan, and H.-H. Wen, arXiv:0804.1726 (unpublished).
[29] K. Hashimoto, T. Shibauchi, T. Kato, K. Ikada, R. Okazaki, H. Shishido, M. Ishikado, H. Kito, A. Iyo, H. Eisaki, S. Shamoto, and Y. Matsuda, Phys. Rev. Lett. **102**, 017002 (2009).
[30] K. Hashimoto, T. Shibauchi, T. Kato, K. Ikada, R. Okazaki, H. Shishido, M. Ishikado, H. Kito, A. Iyo, H. Eisaki, S. Shamoto, and Y. Matsuda, J. Phys. Soc. Jpn. **77**, Suppl. C, 145 (2008).
[31] Z.-A. Ren, G.-C. Che, X.-L. Dong, J. Yang, W. Lu, W. Yi, X.-L. Shen, Z.-C. Li, L.-L. Sun, F. Zhou, and Z.-X. Zhao, Europhys. Lett. **83**, 17002 (2008).
[32] C.-H. Lee, A. Iyo, H. Eisaki, H. Kito, M. T. Fernandez-Diaz, T. Ito, K. Kihou, H. Matsuhata, M. Braden, and K. Yamada, J. Phys. Soc. Jpn. **77**, 083704 (2008).
[33] J. Zhao, Q. Huang, C. de la Cruz, S. Li, J. W. Lynn, Y. Chen, M. A. Green, G. F. Chen, G. Li, Z. Li, J. L. Luo, N. L. Wang, and P. Dai, Nature Mater. **7**, 953 (2008).
[34] E. Zeldov, J. R. Clem, M. McElfresh, and M. Darwin, Phys. Rev. B **49**, 9802 (1994).
[35] T. Shibauchi, M. Konczykowski, C. J. van der Beek, R. Okazaki, Y. Matsuda, J. Yamaura, Y. Nagao, and Z. Hiroi, Phys. Rev. Lett. **99**, 257001 (2007).
[36] M. Konczykowski, L. I. Burlachkov, Y. Yeshurun, and F. Holtzberg, Phys. Rev. B **43**, 13707 (1991).
[37] C. Ren, Z.-s. Wang, H.-q. Luo, H. Yang, L. Shan, and H.-H. Wen, Phys. Rev. Lett. **101**, 257006 (2008).
[38] E. H. Brandt, Phys. Rev. B **60**, 11939 (1999).
[39] H. Luetkens, H.-H. Klauss, M. Kraken, F. J. Litterst, T. Dellmann, R. Klingeler, C. Hess, R. Khasanov, A. Amato, C. Baines, J. Hamann-Borrero, N. Leps, A. Kondrat, G. Behr, J. Werner, and B. Buechner, Phys. Rev. Lett. **101**, 097009 (2008).
[40] R. Okazaki, Y. Kasahara, H. Shishido, M. Konczykowski, K. Behnia, Y. Haga, T. D. Matsuda, Y. Onuki, T. Shibauchi, and Y. Matsuda, Phys. Rev. Lett. **100**, 037004 (2008).
[41] W. K. Kwok, S. Fleshler, U. Welp, V. M. Vinokur, J. Downey, G. W. Crabtree, and M. M. Miller, Phys. Rev. Lett. **69**, 3370 (1992).
[42] Y. Jia, P. Cheng, L. Fang, H. Yang, C. Ren, L. Shan, C.-Z. Gu, and H.-H. Wen, Supercond. Sci. Technol. **21**, 105018 (2008).
[43] V. G. Kogan, Phys. Rev. B **66**, 020509(R) (2002).
[44] P. Miranović, K. Machida, and V. G. Kogan, J. Phys. Soc. Jpn. **72**, 221 (2003).
[45] H. Ding, P. Richard, K. Nakayama, T. Sugawara, T. Arakane, Y. Sekiba, A. Takayama, S. Souma, T. Sato, T. Takahashi, Z. Wang, X. Dai, Z. Fang, G. F. Chen, J. L. Luo, and N. L. Wang, Europhys. Lett. **83**, 47001 (2008).
[46] P. Szabo, Z. Pribulova, G. Pristas, S. L. Bud'ko, P. C. Canfield, and P. Samuely, Phys. Rev. B **79**, 012503 (2009).
[47] K. Hashimoto, T. Shibauchi, S. Kasahara, K. Ikada, T. Kato, R. Okazaki, C. J. van der Beek, M. Konczykowski, H. Takeya, K. Hirata, T. Terashima, and Y. Matsuda, arXiv:0810.3506 (unpublished).
[48] K. Matano, Z. A. Ren, X. L. Dong, L. L. Sun, Z. X. Zhao, and G.-Q. Zheng, Europhys. Lett. **83**, 57001 (2008).
[49] L. Malone, J. D. Fletcher, A. Serafin, A. Carrington, N. D. Zhigadlo, Z. Bukowski, S. Katrych, and J. Karpinski, arXiv:0806.3908 (unpublished).
[50] V. Vildosola, L. Pourovskii, R. Arita, S. Biermann, and A. Georges, Phys. Rev. B **78**, 064518 (2008).
[51] Z. Pribulova, T. Klein, J. Kacmarcik, C. Marcenat, M. Konczykowski, S. L. Budko, M. Tillman, and P. C. Canfield, Phys. Rev. B **79**, 020508(R) (2009).